

Original Article

Time-dependent changes of calbindin D-28K and parvalbumin immunoreactivity in the hippocampus of rats with streptozotocin-induced type 1 diabetes

Sun Shin Yi*

Department of Biomedical Laboratory Science, College of Biomedical Sciences, Soonchunhyang University, Asan 336-745, Korea

The hippocampus is affected by various stimuli that include hyperglycemia, depression, and ischemia. Calcium-binding proteins (CaBPs) have protective roles in the response to such stimuli. However, little is known about the expression of CaBPs under diabetic conditions. This study was conducted to examine alterations in the physiological parameters with type 1 diabetes induced with streptozotocin (STZ) as well as time-dependent changes in the expression of two CaBPs changes of were being evaluated. Rats treated with STZ (70 mg/kg) had high blood glucose levels (>21.4 mmol/L) along with increased food intake and water consumption volumes compared to the sham controls. In contrast, body weight of the animals treated with STZ was significantly reduced compared to the sham group. CB-specific immunoreactivity was generally increased in the hippocampal CA1 region and granule cell layer of the dentate gyrus (DG) 2 weeks after STZ treatment, but decreased thereafter in these regions. In contrast, the number of PV-immunoreactive neurons and fibers was unchanged in the hippocampus and DG 2 weeks after STZ treatment. However, this number subsequently decreased over time. These results suggest that CB and PV expression is lowest 3 weeks after STZ administration, and these deficits lead to disturbances in calcium homeostasis.

Keywords: calbindin D-28K, calcium binding protein, hippocampus, parvalbumin, type I diabetes

Introduction

Recent reports have demonstrated the protective roles of calcium-binding proteins (CaBPs) in response to a variety of conditions that include aging, hyperglycemia, brain ischemia, and depression [9,12,13,15,20,26,30,33]. Among

the CaBPs, calbindin D-28K (CB) and parvalbumin (PV) are primarily found in gamma-aminobutyric acid (GABA)ergic neurons in the hippocampus [9,36]. GABA is the most important inhibitory neurotransmitter in the brain and plays a role in various pathophysiological states [30,33]. These GABAergic and CaBP neuronal markers are believed to participate in a variety of functional brain systems and circuitries. CaBPs are assumed to primarily act in calcium buffering and transport, the regulation of different enzymatic systems [14] and ion channels, and synaptic transmission in the nervous system [1,16]. Several studies have shown that blocking calcium entry through either voltage-gated calcium channels or glutamate receptor antagonists protects the brain from various insults [18,31,35].

Type 1 diabetes mellitus is associated with metabolic, neuronal, endocrine, and immune system alterations at the cellular, tissue, and organ levels [34]. Furthermore, rats with streptozotocin (STZ)-induced type 1 diabetes mellitus were reported to develop hyperglycemia with reduced nerve fiber diameter and myelin width in peripheral tissues [21]. Diabetes involves pathophysiological changes in both the brain and body, and affects reciprocal links between the nervous system and many physiological systems [22]. Likewise, this disease may be a stressor and can perturb hypothalamo-pituitary-adrenal (HPA) axis regulation [38,39].

We hypothesized that GABAergic CaBPs (*e.g.* calbindin D-28K, calretinin and parvalbumin) may play an important role under diabetic conditions. However, few studies of changes in these proteins associated with diabetes, particularly type 1 diabetes, have been conducted. Since chronological alteration of SOD1 activity and inflammatory responses in the hippocampus following STZ administration have been reported [40], we speculated

*Corresponding author: Tel: +82-41-530-4873; Fax: +82-41-530-3085; E-mail: admiral96@sch.ac.kr

that CaBP expression should be modulated in order to maintain brain homeostasis following an insult. We therefore performed this study to examine hippocampal CB and PV expressions in STZ-treated type 1 diabetic rats at various times after disease onset.

Materials and Methods

Experimental animals

Male Wistar rats were purchased from SLC (Shizuoka, Japan). The animals were 8 weeks old and had body weights between 190 and 240 g. The rats were housed at 22°C with 55% humidity and an alternating 12-h light/dark cycle, and had free access to normal chow diet and tap water. The care and handling of the animals conformed to guidelines compliant with the National Institutes of Health Guide for the Care and Use of Laboratory Animals, and were approved by the Institutional Animal Care and Use Committee (IACUC) at Seoul National University, College of Veterinary Medicine (Korea). All experiments were conducted to minimize the number of rats used and animal discomfort.

Treatment with STZ

The rats were divided into four groups (10 animals/ group). One group was treated with citrate buffer (pH 4.3, vehicle) and the other rats were treated with STZ before being evaluated 2, 3, and 4 weeks after treatment (STZ2w, STZ3w, and STZ4w, respectively). Type 1 diabetes mellitus was induced by a single intra-peritoneal (i.p.) injection of 70 mg/kg/5 mL of freshly prepared STZ (Sigma-Aldrich, USA) in 0.1 M sodium citrate buffer (pH 4.3). The vehicle group received an i.p. injection of the same volume of vehicle. After 72 h, 12-h fasting blood glucose levels were monitored. Rats with blood glucose levels exceeding 8.0 mmol/L were defined as having diabetes and were used for the subsequent experiments ($n =$ five in each group).

Physiological data acquisition

Blood was collected weekly from tail veins and blood glucose levels were measured using a validated one-touch basic glucose measurement system (SureStep blood glucose meter; Lifescan, USA). Body weights were also measured weekly. Food intake and water consumption of the sham controls and STZ-treated groups were recorded at 09:00 twice a week.

Tissue processing for histological studies

Animals ($n =$ five in each group) were anesthetized with an i.p. injection of 30 mg/kg Zoletil 50 (Virbac, France) and transcardially perfused with 0.1 M phosphate-buffered saline (PBS, pH 7.4) followed by 4% paraformaldehyde in 0.1 M PBS (pH 7.4). Brain tissues were cryoprotected by incubation with 30% sucrose in PBS overnight prior to

cryosectioning. Serial brain sections (30- μ m thick) in the coronal plane were cut using a cryostat (Leica, Germany). The sections were transferred to six-well plates containing PBS for further processing.

Immunohistochemical analysis of CB and PV

The free-floating brain sections were carefully processed under identical conditions. Tissue sections from each animal ($n =$ five per group) were from an area -3.00 and -4.08 mm posterior to the bregma as determined with a rat atlas [28]. The sections were sequentially treated in room temperature with 0.3% hydrogen peroxide (H_2O_2) in PBS for 30 min and 10% normal goat or rabbit serum in 0.05 M PBS for 30 min. Next, the sections were incubated overnight in mouse anti-CB (1 : 2,000 dilution; Swant, Switzerland), and mouse anti-PV (1 : 5,000 dilution; Swant, Switzerland) antibodies at 4°C, and subsequently exposed to biotinylated goat anti-mouse IgG (1 : 200 dilution; Vector, Burlingame, CA, USA) using an avidin-biotin complex kit (Vector, Burlingame, CA, USA). Antibody binding was visualized with 3, 3'-diaminobenzidine tetrachloride (Sigma-Aldrich, USA) in 0.1 M Tris-HCl buffer (pH 7.2) and mounted on gelatin-coated slides. A negative control test was carried out using pre-immune serum instead of primary antibody to establish immunostaining specificity. No immunoreactivity in any structure was observed in the negative controls.

CB- and PV-positive cells in all groups were assessed using an image analysis system equipped with a computer-based CCD camera and Optimas 6.5 software (CyberMetrics, USA). Cell counts for all of the sections from all rats were averaged. The counts are presented as a percentage relative to the number of cells in the vehicle group.

CB-specific immunoreactivity was also graded. The mean intensity of CB immunostaining in each CB-positive structure was measured according to a gray scale system (light-to-dark signal corresponding to 255 ~ 0). Based on this technique, the level of immunoreactivity was scored as no staining (gray scale value ≥ 200), weakly positive (\pm ; gray scale value 150 ~ 190), moderate (+; gray scale value 100 ~ 149), strong (++; gray scale value 50 ~ 99), and very strong (+++, gray scale value ≤ 50).

Statistical analyses

Data are presented as the mean \pm standard error (SE) for each experiment performed. Differences between the groups were statistically analyzed by a one-way analysis of variance followed by Bonferroni post-hoc test and Duncan's new multiple range method. Significant differences indicated ($p < 0.05$).

Results

Changes in physiological parameters

Body weight: Mean body weight of the vehicle group

continuously increased after injection from 299.8 ± 8.54 g at baseline (0 weeks) to 317.3 ± 8.62 g at 1 week, 337.3 ± 7.58 g at 2 weeks, 362.3 ± 5.39 g at 3 weeks, and 390.2 ± 5.99 g at 4 weeks after treatment. In contrast, body weight of the STZ-treated rats fell from 298.8 ± 7.78 g at baseline to 287.3 ± 7.50 g at 1 week, 278.5 ± 8.29 g at 2 weeks, 256.8 ± 8.49 g at 3 weeks, and 226.7 ± 7.94 g at 4 weeks. Mean body weight of the STZ-treated rats was significantly lower than that of the sham control 1 week after treatment and thereafter ($*p < 0.005$; Fig. 1A).

Blood glucose levels: Blood glucose levels of the vehicle control remained low (< 6.1 mmol/L) throughout the experiment. The STZ-treated animals had significantly higher glucose levels (> 21.4 mmol/L; $p < 0.005$) throughout the entire experiment. Mean glucose levels of the vehicle group at 0, 1, 2, 3, and 4 weeks after treatment were 6.1 ± 0.29 mmol/L, 5.9 ± 0.22 mmol/L, 5.8 ± 0.12 mmol/L, 5.7 ± 0.26 mmol/L, and 5.7 ± 0.34 mmol/L,

respectively, while those of the STZ-treated rats were 5.5 ± 0.52 mmol/L, 21.5 ± 0.58 mmol/L, 21.5 ± 0.58 mmol/L, 23.3 ± 0.56 mmol/L, and 22.8 ± 0.37 mmol/L, respectively (Fig. 1B).

Food intake: Food intake of the vehicle group remained low (< 29.0 g/day) throughout the experiment. However, the STZ-treated rats showed a significant increase ($p < 0.005$ versus the vehicle group) in food intake that peaked at 2 weeks after STZ treatment. Thereafter, food intake gradually decreased over time. Mean food intake at 0, 1, 2, 3, and 4 weeks after vehicle treatment was 24.1 ± 1.57 g, 24.9 ± 1.44 g, 25.9 ± 1.39 g, 27.2 ± 1.13 g, and 28.8 ± 13.5 g, respectively, while that observed 0, 1, 2, 3, and 4 weeks after STZ treatment was 22.3 ± 1.69 g, 34.2 ± 3.16 g, 53.8 ± 3.79 g, 53.3 ± 3.63 g, and 47.5 ± 3.62 g, respectively (Fig. 1C).

Water consumption: Water consumption of the vehicle group steadily increased throughout the experiment. Water

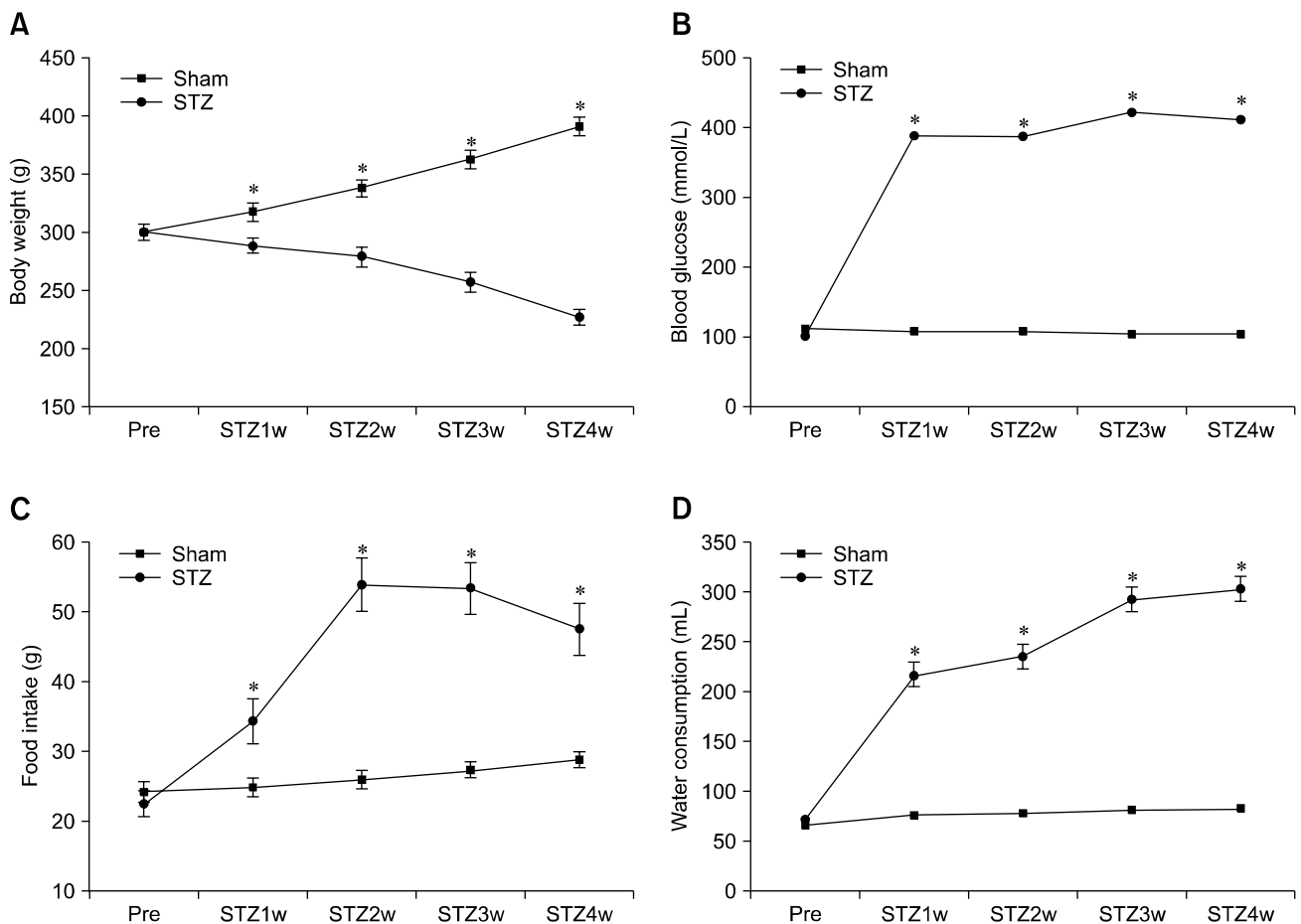


Fig. 1. Physiological data for the sham and streptozotocin (STZ)-treated rats. Body weights of the sham group exponentially increased while those of the STZ-treated rats slowly decreased over the 4-week study period (A). Blood glucose levels at 0, 1, 2, 3, and 4 weeks after STZ treatment (Pre, STZ1w, STZ2, STZ3w, and STZ4w, respectively) were significantly different from those of the sham controls. Blood glucose levels continuously increased in the STZ-treated animals from 21.4 mmol/L 1 week after STZ administration (B). Food intake (C) and water consumption (D) also increased 1 week after STZ treatment. $*p < 0.005$.

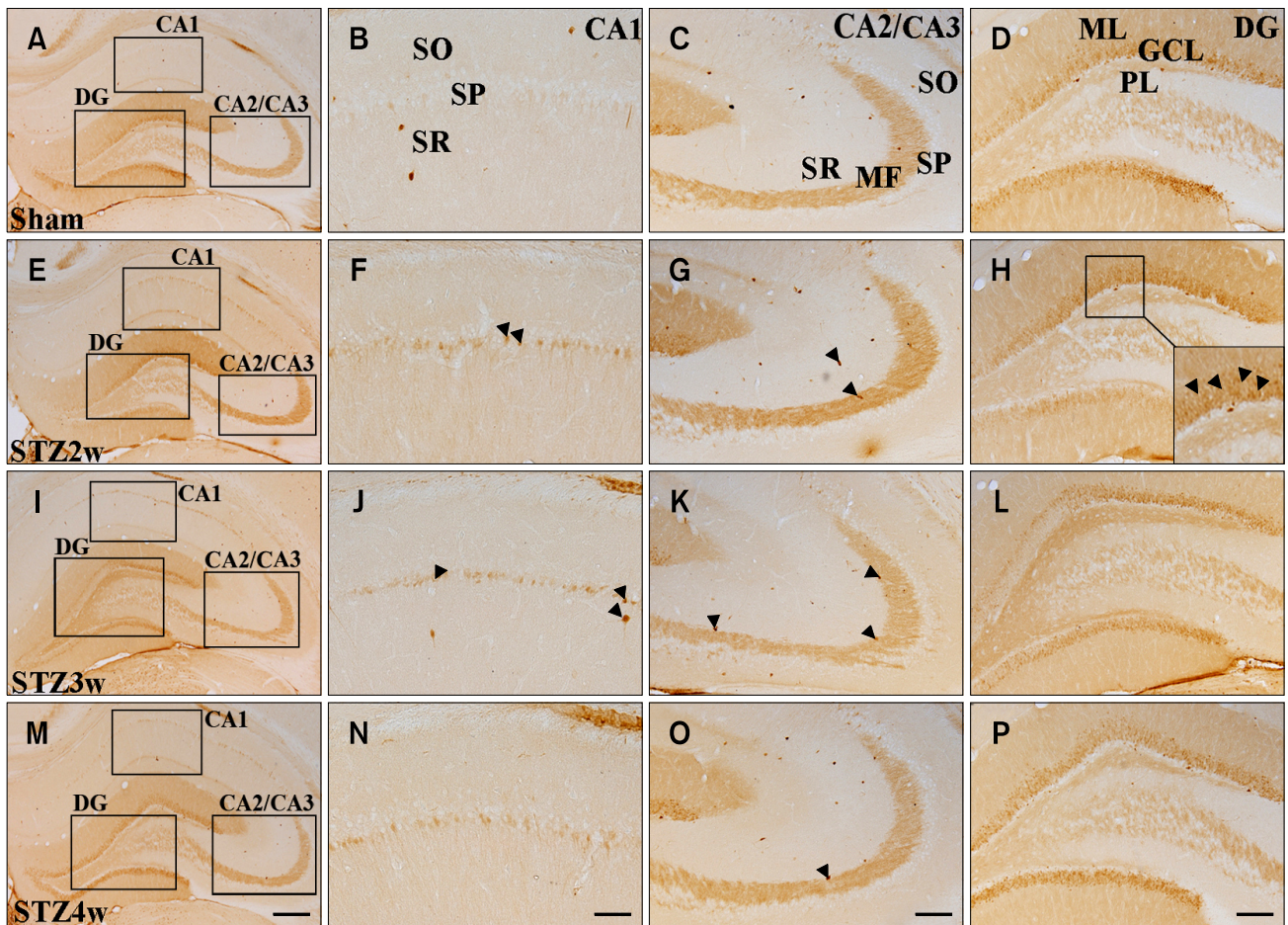


Fig. 2. Immunohistochemical staining for calbindin D-28K (CB) in the hippocampus of sham and STZ-treated rats. The whole hippocampus can be seen in panels A, E, I and M, and the images of the CA1, CA2/CA3, and dentate gyrus (DG) are outlined by black squares. Neurons in the stratum pyramidale were rarely positive in the CA1 regions of the sham controls (B) whereas immunoreactivity observed 2~4 weeks after STZ treatment was stronger (F, J and N). Few CB-positive neurons were observed in the stratum pyramidale of the CA2/CA3; however, CB-specific immunoreactivity in the mossy fibers was strong in all groups (C, G, K and O). Quantification of immunoreactivity in the mossy fibers and granule cell fibers is presented in Table 2. The number of CB-positive cells was decreased 3 weeks after STZ treatment and increased at 4 weeks. Some CB-positive neurons in the CA1 and CA2/CA3 are indicated by black arrowheads in panels F, G, J, K and O. A few CB-positive neurons in the granular cell layer (GCL) of the DG are indicated by black arrowheads in panel H. Time-dependent changes in CaBP-positive staining according to hippocampal region are described in Table 1. GCL: granular cell layer, MF: mossy fiber, ML: molecular layer, PL: polymorphic layer, SO: stratum oriens, SR: stratum radiatum, SP: stratum pyramidale. Scale bars = 100 μ m.

Table 1. Time-dependent changes in CaBP expression according to hippocampal region

CaBP	Group	CA1	CA2/CA3	DG
CB	Sham	7.5 \pm 1.06	–	239.0 \pm 18.27
	STZ2w	32.67 \pm 3.66*	–	235.8 \pm 22.56
	STZ3w	30.67 \pm 4.60*	–	170.3 \pm 16.42*
	STZ4w	29.80 \pm 2.39*	–	197.5 \pm 13.67*
PV	Sham	48.8 \pm 3.80	20.5 \pm 1.26	28.7 \pm 1.87
	STZ2w	24.3 \pm 2.28*	15.5 \pm 1.73*	26.5 \pm 2.40
	STZ3w	22.5 \pm 1.65*	13.8 \pm 0.98*	10.5 \pm 2.6*
	STZ4w	21.1 \pm 2.11*	13.6 \pm 1.15*	24.9 \pm 1.26*

Neuron immunoreactivity (counts) was measured and statistically significant differences are shown (* p < 0.05; vs. the sham). Values are expressed as the mean \pm SE. DG: dentate gyrus, CB: calbindin D-28K, PV: parvalbumin.

consumption of the STZ group dramatically increased compared to that of the vehicle group. Mean water consumption at 0, 1, 2, 3, and 4 weeks after vehicle treatment was 64.3 ± 4.2 mL/day, 73.7 ± 3.88 mL/day, 77.1 ± 4.1 mL/day, 80.2 ± 4.14 mL/day, and 81.0 ± 4.64 mL/day, respectively, while that of the STZ-treated rats at 0, 1, 2, 3, and 4 weeks was 69.2 ± 2.94 mL/day, 215.3 ± 8.77 mL/day, 234.3 ± 8.09 mL/day, 291.7 ± 11.88 mL/day, and 301.8 ± 12.24 mL/day, respectively (Fig. 1D).

Immunohistochemical assays for CB and PV

Changes in CB: In the vehicle and STZ groups, CB-specific immunoreactivity was mainly observed in the granule cell layer of the dentate gyrus (DG) and mossy fibers (Fig. 2). However, some differences in the localization of CB-positive neurons were observed in these regions when comparing the vehicle and STZ groups. There were few CB-positive cells in the hippocampal CA1 region of the vehicle group (Figs. 2A and B) while STZ treatment significantly increased the number of CB-positive cells in the CA1 region at STZ2w (Figs. 2E and F). However, CB-immunoreactive cell populations in the CA1 region were decreased at STZ3w and STZ4w (Figs. 2I, J, M, and N). In the mossy fibers, CB-specific immunoreactivity in the vehicle group was similar to that at STZ2w (Figs. 2A, C, E and G; Table 1) while CB immunoreactivity at STZ3w and STZ4w was significantly decreased in the mossy fibers compared to that in the vehicle group (Figs. 2I and K; Table 2). In the granule cell layer of the DG, the number of CB-positive cells was significantly decreased by 3 weeks after STZ treatment (Table 1) but increased at 4 weeks (Figs. 2A, D, E, H, I, L, M and P).

Changes in PV: In the vehicle and STZ groups, PV-specific immunoreactivity was mainly detected in the nonpyramidal neurons of the hippocampal CA1-3 region and hilar neurons of the DG. PV-positive fibers were also detected in almost all regions of the hippocampus (Fig. 3). However, some differences in the localization of PV-positive neurons and fibers were noted between the vehicle and STZ groups except in the CA2/CA3 region. In the hippocampal CA1

region, the number of PV-positive neurons was significantly decreased in the STZ groups. No significant differences in the number of PV-positive neurons and fibers of the hippocampal CA2/CA3 region were observed when comparing the vehicle and STZ groups (Figs. 3A, C, E, G, I, K, M and O). In the DG, the number of PV-positive neurons and fibers in the vehicle group were similar to that observed at STZ2w (Figs. 3A, D, E and H) while the numbers of PV-immunoreactive neurons and fibers were significantly decreased at STZ3w compared to those in the vehicle group (Figs. 3I and L). At STZ4w, the numbers of PV-positive neurons and fibers increased in the DG to the level of the vehicle group (Figs. 3M and P).

Discussion

CaBPs are thought to play important roles in the maintenance of calcium homeostasis and protection of neurons against various insults [14]. In the present study, we evaluated the expression of two major CaBPs, CB and PV, in the hippocampus. CB-positive neurons were abundant in the CA1 region of the STZ-treated animals and were significantly increased in number compared to the vehicle group although CB expression declined over time.

Several reports have shown that blocking calcium entry either by regulating voltage-gated calcium channels or using glutamate receptor antagonists protects against ischemia, ischemia-like insults, and depression [10,11,19,29,30,31]. Furthermore, limiting intracellular calcium accumulation by administering various chelators protects neurons against excitotoxicity [32,33]. CaBP overexpression also has neuroprotective effects in neurodegenerative models [37]. These findings suggest that the effective regulation of calcium ion movement is closely associated with neuronal survival. However, few studies have been conducted on CaBP levels in the type 1 diabetic brain.

CB-positive neurons are believed to be associated with memory, learning, and long-term potentiation [25]. CB is present in many double bouquets, bitufted, bipolar, multipolar, and horizontal (Cajal-Retzius) cells [2-7] as well as pyramidal and nonpyramidal neurons in the hippocampus [2,12]. Lee et al. reported that younger gerbils (1 month old) show weaker CB expression in the hippocampal CA1 region compared to older gerbils [17]. In the present study, CB-specific immunoreactivity in CA2/CA3 mossy fibers, granule cell fibers, and the DG gradually decreased; however, expression in the DG was increased at STZ4w.

PV-positive cell counts in all regions except the DG were significantly ($p < 0.05$) reduced in the STZ-treated rats 2 ~ 4 weeks after treatment. The number of PV-positive cells in the DG increased after this period. The CA1 and CA2/CA3 regions appeared to be more affected by STZ over time than

Table 2. Time-dependent changes of CB-positive staining in mossy fibers and granule cells in the hippocampus of sham and STZ-treated animals

	Sham	STZ2w	STZ3w	STZ4w
Mossy fibers	+++	+++	++	++
Granule fibers	±	++	+	+

The levels of immunoreactivity were defined as very weakly positive (±), weakly positive (+), moderately positive (++), and strongly positive (+++).

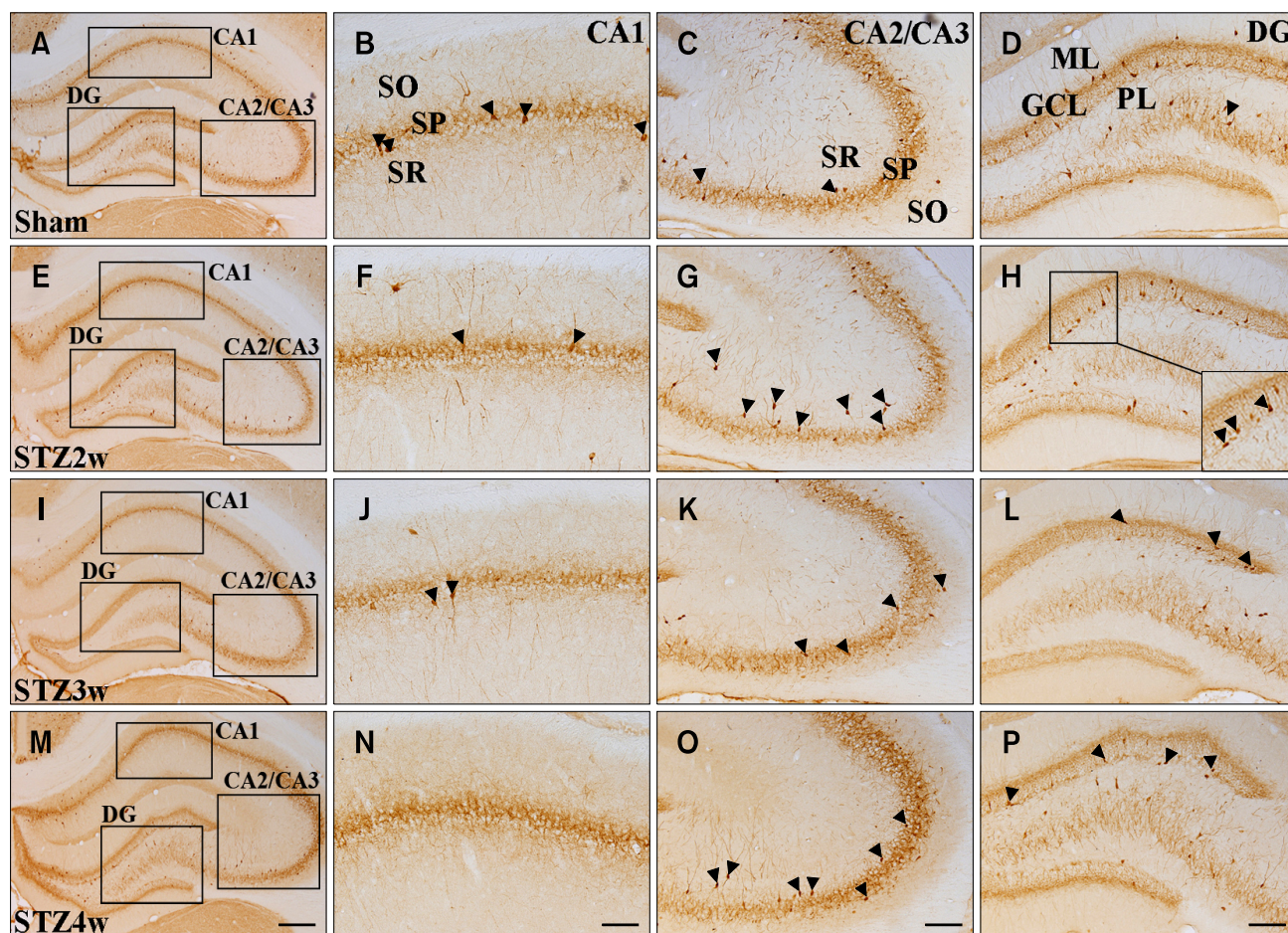


Fig. 3. Immunohistochemical staining for parvalbumin (PV) in the hippocampus of sham and STZ-treated rats. The whole hippocampus can be seen in panels A, E, I and M while images of the CA1, CA2/CA3, and DG are outlined by black squares. PV-positive neurons in the CA1 were observed in the stratum oriens, stratum radiatum, and stratum pyramidale, but were primarily found in the stratum pyramidale (panels B, F, J and N). PV-positive neurons were also found along with the granular cell layer and polymorphic layer of the DG. A few PV-positive neurons in the CA1 and CA2/CA3 are indicated by black arrowheads in panels B, C, F, G, J, K and O. Some CB-positive neurons in the DG are indicated by black arrowheads in panels D, H, L and P. Immunoreactivity specific for PV-positive neurons in the CA1 and CA2/CA3 regions gradually decreased over time (Table 1). Staining in the DG was first significantly reduced 3 weeks after STZ treatment and then rose to the same level found in the sham control at 4 weeks. Scale bars = 100 μ m.

the DG. The CB- and PV-positive cell counts in the DG at STZ4w were significantly increased compared to the sham animals. Previous studies demonstrated that CA1 hippocampal neurons are particularly vulnerable to insults while DG cells are notably resistant [1,8]. In the present study, CB-specific immunoreactivity in the DG changed over time with a tendency to become reduced. Although CaBPs play protective roles, these proteins do not protect against cyanide toxicity, and it has also been suggested that the protective effects of CaBPs do not extend to mitochondrial toxins [37].

It has been reported that the number of CB- and PV-positive neurons are significantly increased in the inner nuclear layers of the retina of rats with STZ-induced diabetes [27]. Increased levels of CB and PV in amacrine and bipolar cells may function as buffering reservoirs that

maintain calcium homeostasis and protect against the damaging effects of excessive calcium influx during over-excitation. Moreover, several studies have indicated that the CaBPs function, in part, as neuroprotective factors because these proteins are localized within nerve cells that are often less vulnerable to degeneration in patients with Alzheimer's or Parkinson's disease [18,23,24]. Although CB expression in the CA1 gradually decreased from 2 weeks to 4 weeks after STZ treatment, the reason why CB immunoreactivity showed strong signals in CA1 at STZ2w could be that CB activation maintained calcium homeostasis and protected the mechanisms mentioned above.

A recent study reported appreciable changes in Cu levels along with Zn-superoxide dismutase (SOD1), 4-hydroxy-2-nonenal (4-HNE), and microglial activities in rat

hippocampus 3 weeks after injection of STZ [40]. Therefore, oxidative stress-related events in the brain of animals with STZ-induced diabetes also seemed to be the most serious and critical at this time point. In the present study, CB and PV expression was reduced 3 weeks after STZ treatment. However, this was restored at 4 weeks in the DG while expression of these proteins in the CA1 and CA2/CA3 were decreased without recovery due to their vulnerability to the STZ toxicity.

In summary, CB and PV expression in the DG was reduced by STZ until 3 weeks after treatment. However, expression of these proteins recovered and increased 4 weeks after treatment. Results from the present study also showed that CB and PV levels were lowest 3 weeks after STZ treatment. Deficits in these proteins at this time point may lead to disturbances in calcium homeostasis.

Acknowledgments

This research supported by the Soonchunhyang University Research Fund.

References

1. **Baimbridge KG, Celio MR, Rogers JH.** Calcium-binding proteins in the nervous system. *Trends Neurosci* 1992, **15**, 303-308.
2. **Celio MR.** Calbindin D-28k and parvalbumin in the rat nervous system. *Neuroscience* 1990, **35**, 375-475.
3. **DeFelipe J, Hendry SHC, Jones EG.** Synapses of double bouquet cells in monkey cerebral cortex visualized by calbindin immunoreactivity. *Brain Res* 1989, **503**, 49-54.
4. **DeFelipe J, Hendry SHC, Hashikawa T, Molinari M, Jones EG.** A microcolumnar structure of monkey cerebral cortex revealed by immunocytochemical studies of double bouquet cell axons. *Neuroscience* 1990, **37**, 655-673.
5. **Demeulemeester H, Vandesande F, Orban GA, Brandon C, Vanderhaeghen JJ.** Heterogeneity of GABAergic cells in cat visual cortex. *J Neurosci* 1988, **8**, 988-1000.
6. **Demeulemeester H, Vandesande F, Orban GA, Heizmann CW, Pochet R.** Calbindin D-28K and parvalbumin immunoreactivity is confined to two separate neuronal subpopulations in the cat visual cortex, whereas partial coexistence is shown in the dorsal lateral geniculate nucleus. *Neurosci Lett* 1989, **99**, 6-11.
7. **Demeulemeester H, Arckens L, Vandesande F, Orban GA, Heizmann CW, Pochet R.** Calcium binding proteins and neuropeptides as molecular markers of GABAergic interneurons in the cat visual cortex. *Exp Brain Res* 1991, **84**, 538-544.
8. **Freund TF, Buzsáki G, Leon A, Baimbridge KG, Somogyi P.** Relationship of neuronal vulnerability and calcium binding protein immunoreactivity in ischemia. *Exp Brain Res* 1990, **83**, 55-66.
9. **Freund RF, Buzsáki G.** Interneurons of the hippocampus. *Hippocampus* 1996, **6**, 347-470.
10. **Gavard JA, Lustman PJ, Clouse RE.** Prevalence of depression in adults with diabetes. An epidemiological evaluation. *Diabetes Care* 1993, **16**, 1167-1178.
11. **Gomez R, Vargas CR, Wajner M, Barros HMT.** Lower in vivo brain extracellular GABA concentration in diabetic rats during forced swimming. *Brain Res* 2003, **968**, 281-284.
12. **Green AR, Hainsworth AH, Jackson DM.** GABA potentiation: a logical pharmacological approach for the treatment of acute ischaemic stroke. *Neuropharmacology* 2000, **39**, 1483-1494.
13. **Grillo CA, Piroli GG, Wood GE, Reznikov LR, McEwen BS, Reagan LP.** Immunocytochemical analysis of synaptic proteins provides new insights into diabetes-mediated plasticity in the rat hippocampus. *Neuroscience* 2005, **136**, 477-486.
14. **Heizmann CW, Braun K.** Changes in Ca²⁺-binding proteins in human neurodegenerative disorders. *Trends Neurosci* 1992, **15**, 259-264.
15. **Hwang IK, Yoo KY, Nam YS, Choi JH, Seo K, Lee IS, Jung JY, Kang TC, Oh YS, Won MH.** Age-related changes in calretinin-immunoreactive periglomerular cells in the rat main olfactory bulb. *J Vet Med Sci* 2006, **68**, 465-469.
16. **Iqbal Z, Ochs S.** Fast axoplasmic transport of a calcium-binding protein in mammalian nerve. *J Neurochem* 1978, **31**, 409-418.
17. **Lee CH, Hwang IK, Yoo KY, Choi JH, Park OK, Lee JC, Jeong YG, Lee IS, Won MH.** Calbindin D-28k immunoreactivity and its protein level in hippocampal subregions during normal aging in gerbils. *Cell Mol Neurobiol* 2009, **29**, 665-672.
18. **Leuba G, Kraftsik R, Saini K.** Quantitative distribution of parvalbumin, calretinin, and calbindin D-28k immunoreactive neurons in the visual cortex of normal and Alzheimer cases. *Exp Neurol* 1998, **152**, 278-291.
19. **Lustman PJ, Griffith LS, Gavard JA, Clouse RE.** Depression in adults with diabetes. *Diabetes Care* 1992, **15**, 1631-1639.
20. **Malone JI, Lowitt S, Korthals JK, Salem A, Miranda C.** The effect of hyperglycemia on nerve conduction and structure is age dependent. *Diabetes* 1996, **45**, 209-215.
21. **Malone JI, Lowitt S, Salem AF, Miranda C, Korthals JK, Carver J.** The effects of acetyl-L-carnitine and sorbinil on peripheral nerve structure, chemistry, and function in experimental diabetes. *Metabolism* 1996, **45**, 902-907.
22. **McEwen BS, Magariños, AM Reagan LP.** Studies of hormone action in the hippocampal formation possible relevance to depression and diabetes. *J Psychosom Res* 2002, **53**, 883-890.
23. **McMahon A, Wong BS, Iacopino AM, Ng MC, Chi S, German DC.** Calbindin-D28k buffers intracellular calcium and promotes resistance to degeneration in PC12 cells. *Brain Res Mol Brain Res* 1998, **54**, 56-63.
24. **Mikkonen M, Alafuzoff I, Tapiola T, Soininen H, Miettinen R.** Subfield- and layer-specific changes in parvalbumin, calretinin and calbindin-D28K immunoreactivity in the entorhinal cortex in Alzheimer's disease. *Neuroscience* 1999, **92**, 515-532.
25. **Molinari S, Battini R, Ferrari S, Pozzi L, Killcross AS, Robbins TW, Jouvenceau A, Billard JM, Dutar P,**

- Lamour Y, Baker WA, Cox H, Emson PC.** Deficit in memory and hippocampal long-term potentiation in mice with reduced calbindin D28K expression. *Proc Natl Acad Sci U S A* 1996, **93**, 8023-8033.
26. **Nam SM, Kim YN, Yoo DY, Yi SS, Kim W, Hwang IK, Seong JK, Yoon YS.** Hypothyroid states mitigate the diabetes-induced reduction of calbindin D-28k, calretinin, and parvalbumin immunoreactivity in type 2 diabetic rats. *Neurochem Res* 2012, **37**, 253-260.
 27. **Ng YK, Zeng XX, Ling EA.** Expression of glutamate receptors and calcium-binding proteins in the retina of streptozotocin-induced diabetic rats. *Brain Res* 2004, **1018**, 66-72.
 28. **Paxinos G, Watson C.** *The Rat Brain: In Stereotaxic Coordinates*. 3rd ed. pp. 30-33, Elsevier Academic Press, Amsterdam, 2007.
 29. **Perez-Pinzon MA, Yenari MA, Sun GH, Kunis DM, Steinberg GK.** SNX-111, a novel, presynaptic N-type calcium channel antagonist, is neuroprotective against focal cerebral ischemia in rabbits. *J Neurol Sci* 1997, **153**, 25-31.
 30. **Petty F.** GABA and mood disorders: a brief review and hypothesis. *J Affect Disord* 1995, **34**, 275-281.
 31. **Rothman SM, Olney JW.** Excitotoxicity and the NMDA receptor - still lethal after eight years. *Trends Neurosci* 1995, **18**, 57-58.
 32. **Scharfman HE, Schwartzkroin PA.** Protection of dentate hilar cells from prolonged stimulation by intracellular calcium chelation. *Science* 1989, **246**, 257-260.
 33. **Shiah IS, Yatham LN.** GABA function in mood disorders: an update and critical review. *Life Sci* 1998, **63**, 1289-1303.
 34. **Sposato V, Manni L, Chaldakov GN, Aloe L.** Streptozotocin-induced diabetes is associated with changes in NGF levels in pancreas and brain. *Arch Ital Biol* 2007, **145**, 87-97.
 35. **Steinberg GK, Panahian N, Pérez-Pinzón MA, Sun GH, Modi MW, Sepinwall J.** Narrow temporal therapeutic window for NMDA antagonist protection against focal cerebral ischemia. *Neurobiol Dis* 1995, **2**, 109-118.
 36. **Yanovsky Y, Schubring SR, Yao Q, Zhao Y, Li S, May A, Haas HL, Lin JS, Sergeeva OA.** Waking action of ursodeoxycholic acid (UDCA) involves histamine and GABAA Receptor Block. *PLoS One* 2012, **7**, e42512.
 37. **Yenari MA, Minami M, Sun GH, Meier TJ, Kunis DM, McLaughlin JR, Ho DY, Sapolsky RM, Steinberg GK.** Calbindin D28K overexpression protects striatal neurons from transient focal cerebral ischemia. *Stroke* 2001, **32**, 1028-1035.
 38. **Yi SS, Hwang IK, Kim YN, Kim IY, Pak SI, Lee IS, Seong JK, Yoon YS.** Enhanced expressions of arginine vasopressin (Avp) in the hypothalamic paraventricular and supraoptic nuclei of type 2 diabetic rats. *Neurochem Res* 2008, **33**, 833-841.
 39. **Yi SS, Hwang IK, Chun MS, Kim YN, Kim IY, Lee IS, Seong JK, Yoon YS.** Glucocorticoid receptor changes associate with age in the paraventricular nucleus of type II diabetic rat model. *Neurochem Res* 2009, **34**, 851-858.
 40. **Yi SS, Hwang IK, Kim DW, Shin JH, Nam SM, Choi JH, Lee CH, Won MH, Seong JK, Yoon YS.** The chronological characteristics of SOD1 activity and inflammatory response in the hippocampi of STZ-induced type 1 diabetic rats. *Neurochem Res* 2011, **36**, 117-128.